Bioorg. Med. Chem. Lett. 37 (2021) 127838

Contents lists available at ScienceDirect

Bioorganic & Medicinal Chemistry Letters

journal homepage: www.elsevier.com/locate/bmcl

Discovery and optimization of a novel CNS penetrant series of $mGlu_4$ PAMs based on a 1,4-thiazepane core with *in vivo* efficacy in a preclinical Parkinsonian model

Caitlin N. Kent [a,b,1], Mark G. Fulton [a,b,1], Kaylee J. Stillwell [a,b], Jonathan W. Dickerson [a,b], Matthew T. Loch [a,b], Alice L. Rodriguez [a,b], Anna L. Blobaum [a,b], Olivier Boutaud [a,b], Jerri L. Rook [a,b], Colleen M. Niswender [a,b,d,e], P. Jeffrey Conn [a,b,d,e], Craig W. Lindsley [a,b,c,e,*]

[a] Warren Center for Neuroscience Drug Discovery, Vanderbilt University, Nashville, TN 37232, USA
[b] Department of Pharmacology, Vanderbilt University School of Medicine, Nashville, TN 37232, USA
[c] Department of Chemistry, Vanderbilt University, Nashville, TN 37232, USA
[d] Vanderbilt Kennedy Center, Vanderbilt University Medical Center, Nashville, TN 37232, USA
[e] Vanderbilt Institute of Chemical Biology, Vanderbilt University, Nashville, TN 37232, USA

ARTICLE INFO

Keywords:
$mGlu_4$
Metabotropic glutamate receptor
Positive allosteric modulator (PAM)
Structure-activity-relationship (SAR)

ABSTRACT

A high throughput screen (HTS) identified a novel, but weak (EC_{50} = 6.2 μM, 97% Glu Max) $mGlu_4$ PAM chemotype based on a 1,4-thiazepane core, VU0544412. Reaction development and chemical optimization delivered a potent $mGlu_4$ PAM VU6022296 (EC_{50} = 32.8 nM, 108% Glu Max) with good CNS penetration (K_p = 0.45, $K_{p,uu}$ = 0.70) and enantiopreference. Finally, VU6022296 displayed robust, dose-dependent efficacy in reversing Haloperidol-Induced Catalepsy (HIC), a rodent preclinical Parkinson's disease model.

Introduction

The effective, long-term treatment of Parkinson's disease (PD) remains a significant healthcare challenge, and due to both non-motor symptoms that develop over time, as well as dyskinesia issues with dopamine replacement therapy, a non-dopaminergic approach is needed.[1–6] Selective activation of the metabotropic glutamate receptor subtype 4 (mGu_4), by virtue of positive allosteric modulators (PAMs), has been shown to significantly reduce and/or eliminate motor symptoms in preclinical models of PD by decreasing output of the indirect pathway in the basal ganglia, akin to deep brain stimulation (DBS).[7–15] A number of $mGlu_4$ PAM chemotypes **1**–**5** have demonstrated preclinical efficacy in PD models (Fig. 1), but only recently has an $mGlu_4$ PAM (Prexton Therapeutics Foliglurax®, **6**) entered clinical development.[15–19] However, the chemical landscape for $mGlu_4$ PAMs has been largely dominated by flat, highly sp^2-hybridized molecules that engender poor solubility, formulation challenges or possess undesirable chemical moieties.[7–19] Based on these chemotype-driven, physiochemical challenges, we sought to identify $mGlu_4$ PAMs based on new, sp^3-enriched chemotypes in hopes that more attractive overall profiles would result. Towards this end, we performed a high-throughput screen (HTS), initially employing an $mGlu_{2/4}$ heterodimer HEK293 cell line with native coupling to G protein-coupled inwardly-rectifying potassium channels, or GIRK (using thallium flux as a read-out), followed by a homomeric $mGlu_4$ counter-screen.[20] This screening exercise identified a novel $mGlu_4$ PAM chemotype based on an sp^3-hybridized 1,4-thiazepane core, which was

Multiple domains of VU0544412 (**7**) were explored chemically in search of the optimal $mGlu_4$ PAM within this unique series (Fig. 2). Elements of interest included the stereochemistry at the C-3 center (the HTS hit was 3-(*R*), derived from L-cysteine), ring contracted variants, replacement of the sulfur with carbon or oxygen and a diverse amide scan.

Synthesis of the 1,4-thiazepane core initially was attempted following the only literature report, a 1971 protocol by Blondeau and coworkers (Scheme 1).[21] Here, methyl acrylate **9** underwent a 1,4-addition with L-cysteine **10** to deliver thioether **11** in 88% yield. Intramolecular cyclization to form the 1,4-thiazepane **12** proceeded in the presence of 7

* Corresponding author.
E-mail address: craig.lindsley@vanderbilt.edu (C.W. Lindsley).
[1] These authors contributed equally

https://doi.org/10.1016/j.bmcl.2021.127838
Received 4 January 2021; Received in revised form 25 January 2021; Accepted 30 January 2021
Available online 5 February 2021

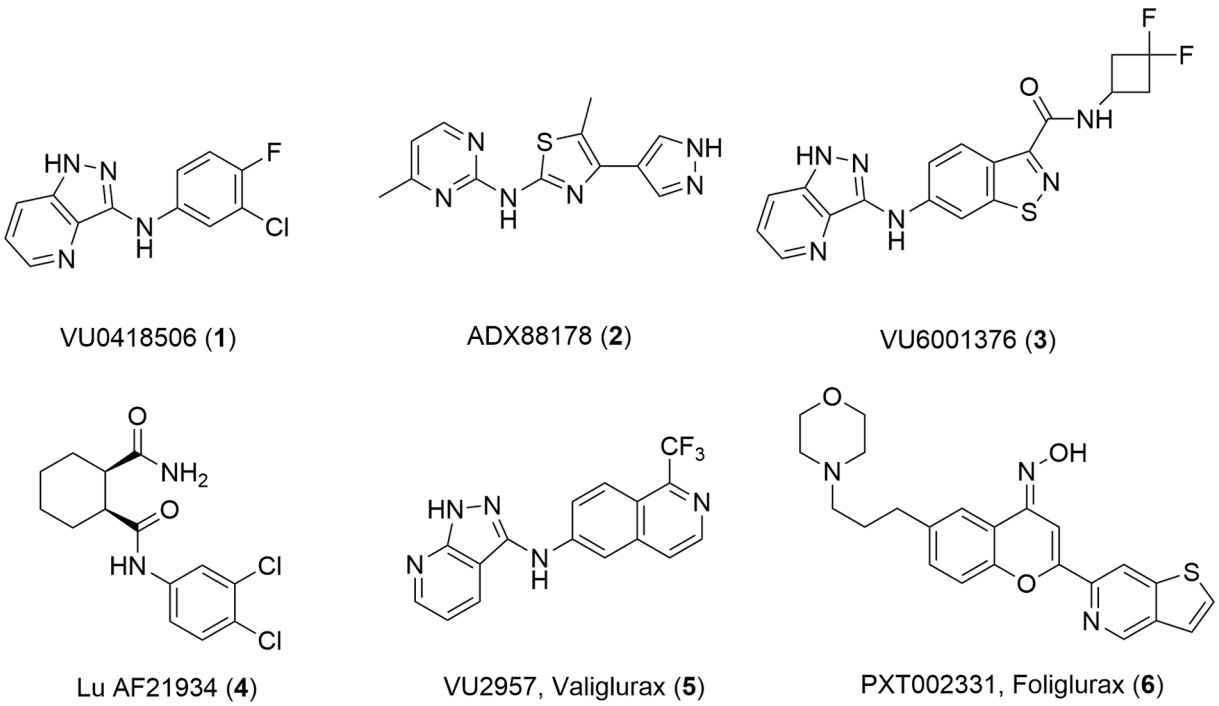

Fig. 1. Structures of prototypical $mGlu_4$ PAMs **1**–**5** and **6** (Foliglurax), the first $mGlu_4$ PAM to advance into human clinical studies. Optimized into a CNS penetrant tool compound with *in vivo* efficacy in the rat haloperidol-induced catalepsy (HIC) model.

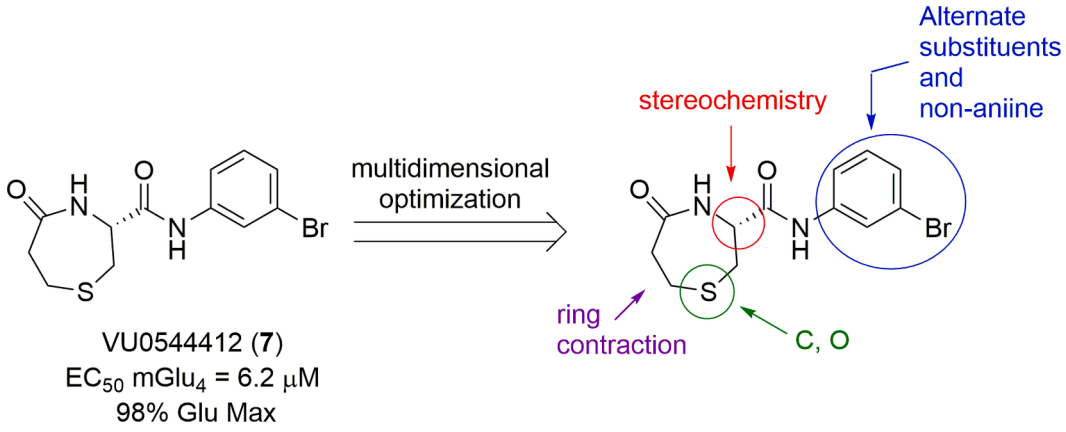

Fig. 2. Multi-dimensional optimization plan for the HTS hit $mGlu_4$ PAM **7**.

N NH_3/MeOH for seven days, resulting in low conversion (13%). With the acid in hand, HATU-mediated amide coupling with diverse anilines delivered amide congeners **13** in yields ranging from 5 to 15%. Yields were modestly better with non-aromatic amines, but these proved inactive as $mGlu_4$ PAMs. The yields from this route were not sufficient to drive a hit-to-lead campaign, so the team paused to improve the synthetic route.

While little literature precedent exists for the preparation of substituted 1,4-thiazepines as chemical probes, there are several works that report 1,4-thiazepines as a byproduct of a fluorescent cysteine detection system; thus, we hijacked and evaluated this application.[22,23] Here (Scheme 2), we employed the fluorescent probe 2-(2′-hydroxy-4′-methoxyphenyl)benzo-thiazole (HMBT) **15**, readily prepared from aldehyde **14** in 91% yield. Treatment of **15** with acroyl chloride smoothly delivers key substrate **16** in 89% yield. Exposure of **16** with L-cysteine **10** facilitates a conjugate addition/cyclization cascade to provide the desired **12** in 62% yield, along with recovered HMBT that could be re-acylated and recycled to produce more **12**. Finally, carbodiimide couplings employing DIC/HOBt proved optimal with **12**, delivering final analogs **13** in yields ranging from 35 to 70%. While superior to our initial route and enabled early SAR, this was not suitable for scale-up chemistry to provide sufficient compound quantities for *in vivo* studies.

We next revisited the initial strategy, but replaced methyl acrylate **9** with acrylic acid (Scheme 3). Conjugate addition of **10** into acrylic acid proceeded quickly in one hour giving **11** in 60% yield. Facilitation of the macrolactamization with HATU provided the methyl ester of **12** in good yield, followed by a mild saponification procedure ($Ba(OH)_2$, THF:H_2O) to produce **12** in 37% overall yield.

With methods in hand for both small and large scale synthesis of analogs **13**, the stage was set for SAR evaluation. As mentioned earlier, only aniline-based amides displayed $mGlu_4$ PAM activity (aliphatic, benzyl and heteroaryl amines were all inactive), and the nature and position of substituents was equally crucial for PAM activity. As shown in Table 1, the HTS hit, with a 3-Br anilino amide **7** was a weak $mGlu_4$ PAM (EC_{50} = 6.2 μM, 98% Glu Max); however, substitution with a chlorine atom, as in **13a**, significantly improved PAM activity (EC_{50} =

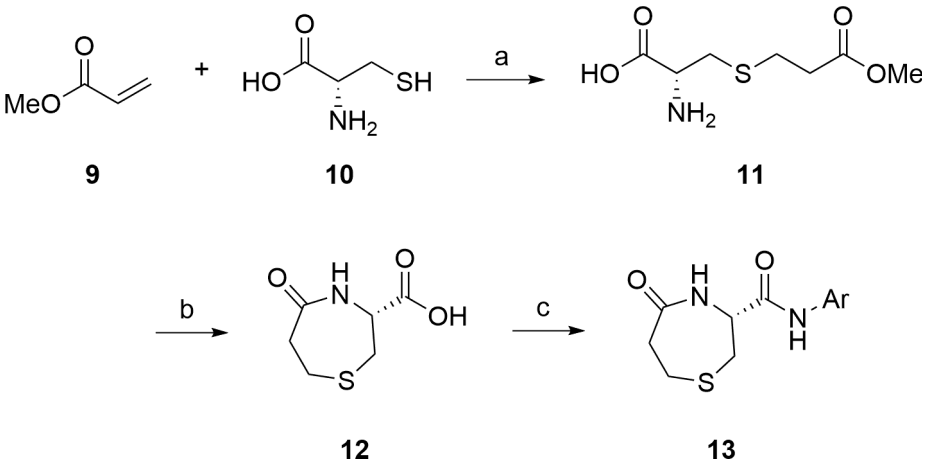

Scheme 1. Synthesis of analogs **13** of the $mGlu_4$ PAM **7**.[a]. [a]*Reagents and conditions*: (a) NEt_3, EtOH, 5 min, rt, 88%; (b) 7 M NH_3/MeOH, 7 days, rt, 13%; (c) HATU, DIPEA, $ArNH_2$, DMF, rt, 12 h, 5–15%.

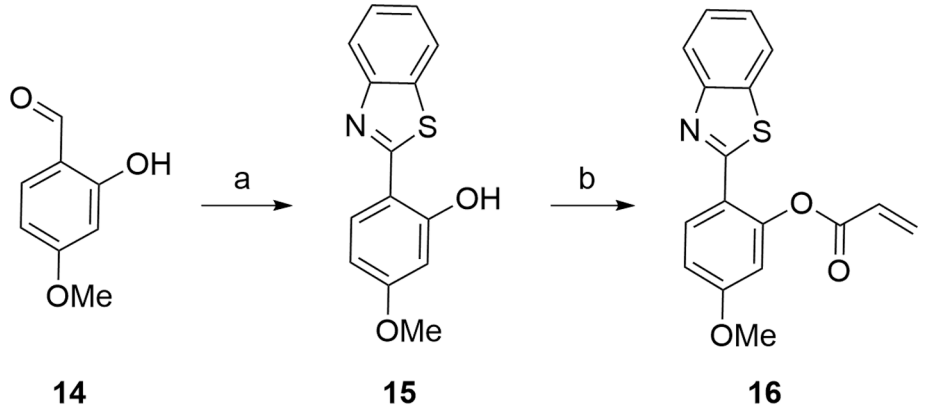

Scheme 2. Alternate synthetic strategy to access **12**[a]. [a]*Reagents and conditions*: (a) 2-Aminobenzenethiol, $AgNO_3$ (1 mol%), DMSO, 1 h, rt, 91%; (b) acroyl chloride, NEt_3, DCM, 12 h, rt, 89%; (c) **10**, DMC, 1 h, rt, 1 h, then DIEPA, 62%; (d) DIC, HOBt, $ArNH_2$, DCM, 1–6 h, rt, 35–70%.

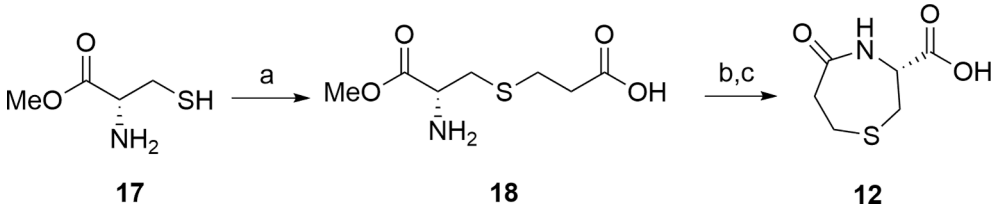

Scheme 3. Synthesis of 1,4-thiazepane core **12** of the $mGlu_4$ PAM **7**.[a]. [a]*Reagents and conditions*: (a) acrylic acid, DIEPA, DCM, 1 h, rt,; (b) HATU, 1 h, rt; (c) $Ba(OH)_2$, THF, H_20, 3 h, rt, 37% over three steps .

148 nM, 120% Glu Max) by > 40-fold. Assuming smaller was better, the 3-F congener was prepared, but inactive, as well as a 3,5-diF derivative, **13b**, which was weaker than the HTS hit. Interestingly, the 3-Cl, 5-F analog **13c**, regained PAM potency (EC_{50} = 278 nM, 112% Glu Max), and a related 3,5-diCl congener proved equipotent (EC_{50} = 273 nM, 88% Glu Max). As a bioisosteric replacement, we surveyed the 3,5-diMe

Table 1

Structure and $mGlu_4$ PAM activities of analogs **13**.

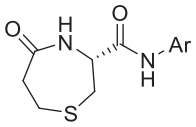

13

Compound	Ar	$mGlu_4$ EC_{50} (nM)	% Glu Max
7	3-Br	6,200	98
13a	3-Cl	148	120
13b	3,5-diF	8,900	102
13c	3-Cl, 5-F	278	112
13d	3-Br, 5-F	351	101
13e	3-I, 5-F	558	102
13f	3,5-diCl	273	88
13g	3-Br, 5-Cl	33	108
13h	3,5-diBr	35	97
13i	3-I, 5-Br	115	101
13j	3,5-diMe	>10	<30
13k	3-Cl, 5-Me	1,090	87
13l	3,5-diCF_3	950	102

[a]Thallium mobilization assays with HEK293/GIRK cells co-expressing rat $mGlu_4$ performed in the presence of an EC_{20} fixed concentration of glutamate; values represent N = 1 experiment performed in triplicate.

variant **13j**, and surprisingly, this compound was devoid of $mGlu_4$ PAM activity. Whereas the 3-Br HTS hit **7** was weak, unexpectedly, a 3,5-diBr analog **13h** was extremely potent (EC_{50} = 35 nM, 97% Glu Max) as was a 3-Br, 5-Cl derivative **13g** (EC_{50} = 33 nM, 108% Glu Max). All other analogs **13** were notably weaker, and replacement of the sulfur atom with either an oxygen atom (e.g., an oxo-1,4-oxazepane) or a methylene group (e.g., a 7-oxoazepane) led to inactive compounds as well.

The importance of the (*R*)-stereochemistry at C3 had yet to be evaluated, thus, following the route in Scheme 3, but substituting D-cysteine, representative (*S*)-analogs **19** were prepared and evaluated (Fig. 3). The (*S*)-analog **19a** of **7** was inactive, whereas the (*S*)-analogs of **13g** and **13h**, **19b** and **19c**, respectively, were ~ 2-fold less potent (EC_{50}s of 64 nM and 76 nM, respectively). Therefore, the (*R*)-enantiomer was favored, yet viable tools could potentially still be obtained with the opposite enantiomer. Contraction to 6-membered rings, of either stereochemistry, proved devoid of $mGlu_4$ PAM activity.

We then evaluated the representative analogs **13** (**13a**, **13g** and **13h**) in a battery of in vitro and *in vivo* DMPK assays (Table 2) to determine if the potent $mGlu_4$ PAMs discovered within this novel chemotype had the profiles necessary to serve as *in vivo* tool compounds. PAM **13a**, the 3-Cl analog, was a low molecular weight compound (MW = 284), with a low cLogP (1.52), high predicted hepatic clearance in rat (CL_{hep} = 63.6 mL/min/kg), but moderate in human (CL_{hep} = 9.4 mL/min/kg) and with acceptable free fraction (f_us 0.02 – 0.03). However, in a rat plasma and brain level (PBL) tissue distribution cassette, **13a** was not CNS penetrant, showing no detectable drug levels in the brain, in agreement with the low cLogP. In contrast, **13h**, a 3,5-diBr analog displayed a cLogP of 2.28, and a brain-to-plasma partitioning coefficient (K_p) of 0.19 (unbound $K_{p,uu}$ = 0.10), suggesting, that in this series, cLogP is a reasonable predictor of K_p. This hypothesis was further borne out by **13g**, a 3-Br, 5-Cl congener, with a cLogP of 2.41, and an improved K_p of 0.45 ($K_{p,uu}$ = 0.70). Moreover, **13g** (VU6022296) was predicted to be moderately cleared in both human and rat (13.1 mL/min/kg and 59.9 mL/min/kg, respectively), with acceptable unbound fraction in both plasma and brain homogenates (human f_u = 0.011, rat f_u = 0.018, rat BHB f_u = 0.028). Thus, **13g** emerged as a reasonable candidate for an *in vivo* tool within this series, and it proved to be highly selective for $mGlu_4$ as well (>10 μM versus $mGlu_{1,2,3,5,7}$ and no inhibition > 50%@10 μM in a radioligand binding panel of 68 GPCRs, ion channels, transporters, and nuclear hormones).[24] **13g** also showed enhance solubility (6.2 μM), versus a prototypical PAM **3**, with kinetic solubility of 0.9 μM.

Based on the potency, selectivity and DMPK profile of **13g**,[25] it was an advanced into a haloperidol-induced catalepsy (HIC) study, a preclinical Parkinsonian rodent model (Fig. 4).[16,18,19] In this study, the vehicle group treated with haloperidol resulted in catalepsy as determined by an increase in the mean latency to withdraw from 0 *sec* to 49.8 *sec*. Treatment with VU6022296 (**13g**) or VU0418506 (VU506, **1**) significantly reduced the mean latency to withdraw in these animals (One-way ANOVA, $F_{4,45}$ = 7.97p < 0.0001). The administration of the positive control VU506 (**1**) significantly reduced cataleptic behavior by 64.0% (mean latency to withdraw 17.9 ± 3.7 s; Fig. 4; ***p < 0.001). The injection of 3 mg/kg of **13g** demonstrated a non-significant reduction of catalepsy by 26.5% (mean latency to withdraw 36.6 ± 4.7 s; p > 0.05). The administration of 10 and 30 mg/kg of **13g** significantly reduced catalepsy by 42.6% and 55.4% (mean latency to withdraw 28.6 ± 5.4 s and 22.2 ± 4.6 s; **p < 0.01, ***p < 0.001). Thus, akin to $mGlu_4$ PAMs in other chemical series and based on other sp^2-centric chemotypes,[16,18,19] potentiation of $mGlu_4$ by this novel 1,4-thiazepane-based PAM series results in robust efficacy in this preclinical model of Parkinson's disease.

In summary, an HTS campaign identified a fundamentally new $mGlu_4$ PAM chemotype based on a 1,4-thiazepane core with weak PAM

Table 2
In vitro and *in vivo* DMPK Profiles of Selected Analogs **13.**

Property	13a	13g	13h
MW	284	363	408
cLogP	1.52	2.41	2.28
tPSA	58	58	58
In vitro PK parameters			
CL_{HEP} (mL/min/kg), rat	63.6	59.9	58.1
CL_{HEP} (mL/min/kg), human	9.4	13.1	12.1
Rat fu_{plasma}	0.02	0.018	0.011
Human fu_{plasma}	0.03	0.011	0.007
Rat fu_{brain}	0.01	0.028	0.006
In vivo Parameters Rat IV PBL cassette (0.2 mg/kg)			
K_p	N/A	0.45	0.19
$K_{p,uu}$	N/A	0.70	0.10

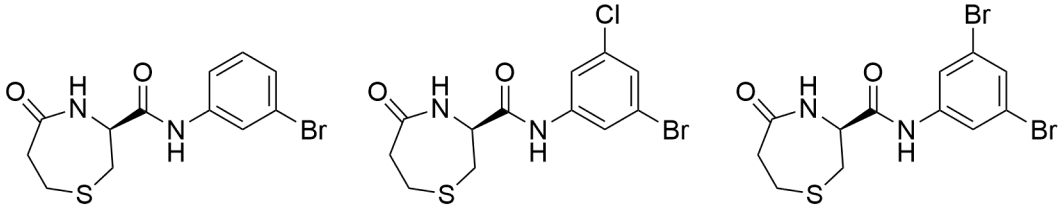

19a $mGlu_4$ EC_{50} >30 μM

19b $mGlu_4$ EC_{50} = 64 nM (98% Glu Max)

19c $mGlu_4$ EC_{50} = 76 nM (104% Glu Max)

Fig. 3. Examples of the activity of the (*S*)-enantiomers **19**.

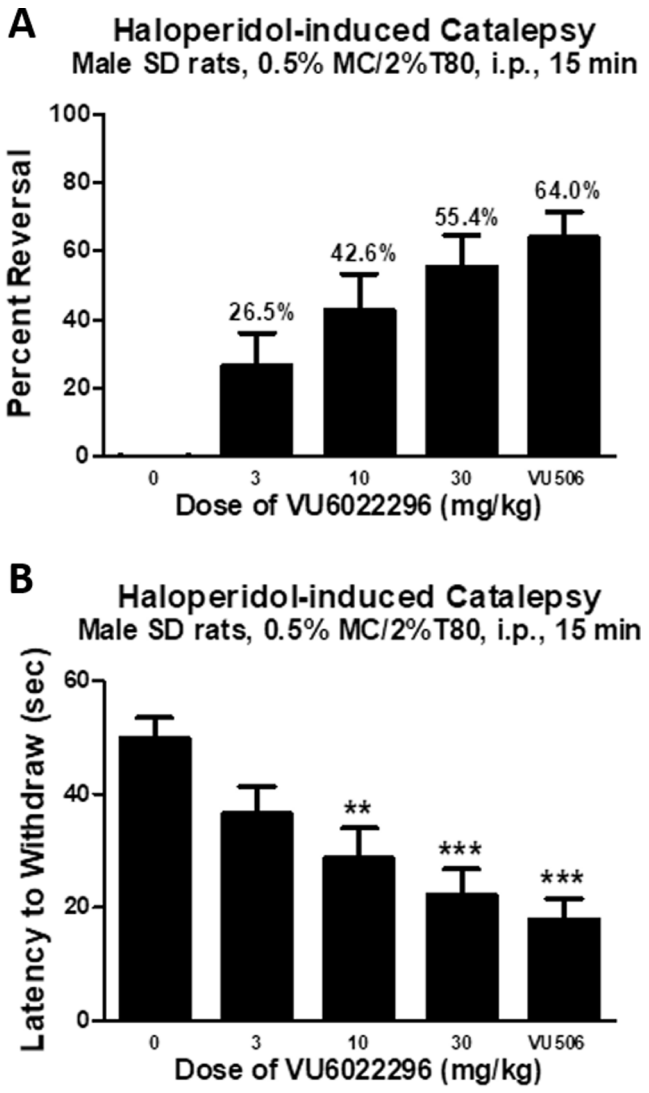

Fig. 4. VU6022296 (**13 g**) dose dependently reduces haloperidol-induced catalepsy in rats. **A**) data shown as percent reversal and **B**) data shown as latency to withdraw. The administration of VU6022296 (**13 g**) significantly reduced mean latency to withdraw at 10 and 30 mg/kg as compared to vehicle-treated controls. The 30 mg/kg dose reversed haloperidol-induced catalepsy to a similar level of the positive control VU0418506, VU506 (**1**). Statistical analysis was performed using a one way ANOVA with Dunnett's post hoc. **p < 0.01, ***p < 0.001 compared to vehicle treated control animals. N = 10 per dosing group.

potency, significant sp^3 character and no detectable CNS penetration. Chemical optimization improved potency by ~ 200-fold, afforded good brain penetration in rat (K_p and $K_{p,uu}$) and showed dose-dependent efficacy in haloperidol-induced catalepsy, a preclinical model of Parkinson's disease. Thus, VU6022296 (**13g**) is a novel in vitro and *in vivo* $mGlu_4$ PAM tool compound. Further exploration of this unique $mGlu_4$ PAM chemotype is underway and will be reported in due course.

Declaration of Competing Interest

The authors declare that they have no known competing financial interests or personal relationships that could have appeared to influence the work reported in this paper.

Acknowledgments

We thank the Warren Family and Foundation for establishing the William K. Warren, Jr. Chair in Medicine (C.W.L.) and endowing the Warren Center for Neuroscience Drug Discovery.

References

1 Lindsley CW, Hopkins CR. *Exp Opin Ther Patent.* 2012;22:461–481.
2 Robichaud AJ, Engers DW, Lindsley CW, et al. *ACS Chem Neurosci.* 2011;2:433–449.
3 Lindsley CW, Emmitte KA, Hopkins CR, et al. *Chem Rev.* 2016;116:6707–6741.
4 Marino MJ, Hess JF, Liverton N. *Curr Top Med Chem.* 2005;5:885–895.
5 Battaglia G, Busceti CL, Molinaro G, et al. *J Neurosci.* 2006;26:7222–7229.
6 Hopkins CR, Lindsley CW, Niswender CM. *Future Med Chem.* 2009;1:501–513.
7 Maj M, Bruno V, Dragic Z, et al. *Neuropharmacology.* 2003;45:895–906.
8 Williams R, Zhou Y, Niswender CM, et al. *ACS Chem Neurosci.* 2010;1:411–419.
9 Kalinichev M, Le Poul E, Bolea C, et al. *J Pharmacol Exp Ther.* 2014;350:495–505.
10 Bennouar KE, Uberti MA, Melon C, et al. *Neuropharmacology.* 2013;66:158–169.
11 Engers DW, Niswender CM, Weaver CD, et al. *J Med Chem.* 2009;52:4115–4118.
12 Engers DW, Blobaum AL, Gogliotti RD, et al. *ACS Chem Neurosci.* 2016;7:1192–1200.
13 Niswender CM, Jones CK, Lin X, et al. *ACS Chem Neurosci.* 2016;7:1201–1211.
14 Hong S-P, Liu KG, Ma G, et al. *J Med Chem.* 2011;54:5070–5081.
15 Engers DW, Bollinger SR, Engers JL, et al. *Bioorg Med Chem Lett.* 2018;28:2641–2646.
16 Bolinger SR, Engers DW, Panarese JD, et al. *J Med Chem.* 2019;62:342–358.
17 https://parkinsonsnewstoday.com/2017/07/28/prexton-initiates-new-phase-2-trial-foliglurax-parkinsons-disease/.
18 Panarese JD, Engers DW, Wu YJ, et al. *ACS Med Chem Lett.* 2019;10:255–265.
19 Panarese JD, Engers DW, Wu YJ, et al. *Bioorg Med Chem Lett.* 2019;29:342–346.
20 Fulton MG, Loch MT, Rodriguez AL, et al. *Bioorg Med Chem Lett.* 2020;30:127212.
21 Blondeau P, Gauthier R, Berse C, et al. *Can J Chem.* 1971;49:3866–3876.
22 Wang J, Li B, Zhao W, et al. *ACS Sens.* 2016;1:882–887.
23 Liu H, Wang X, Xiang Y, et al. *Anal Methods.* 2015;7:5028–5033.
24 See, https://www.eurofinsdiscoveryservices.com/catalogmanagement/viewitem/LeadProfilingScreen-Panel/PP68.
25 Synthesis of 13g: (R)-N-(3-bromo-5-chlorophenyl)-5-oxo-1,4-thiazepane-3-carboxamide. (R)-5-oxo-1,4-thiazepane-3-carboxylic acid (12).To a 100 mL flask, 16 (0.3 mmol) and L-cysteine (0.375 mmol, 1.25 eq) were combined in 3 mL of DCM, and the mixture stirred at rt for 2 h. Then, Et3N (80 μL) was added and the solution stirred for 40 min. The reaction mixture under reduced pressure and the crude solid was subjected to column chromatography to afford 75 mg of HMBT 15 and 39 mg of 12 as an off-white solid. 1H NMR (400 MHz, MeOD) δ 4.54 (dd, J = 8.1, 2.0 Hz, 1H), 3.10 (dd, J = 14.5, 2.0 Hz, 1H), 3.01 – 2.83 (m, 3H), 2.78 – 2.69 (m, 2H). 13C NMR (101 MHz, MeOD) δ 177.15, 170.87, 57.53, 40.65, 33.48, 23.70. LC-MS [m/z+H] = 176.3. Analytical data are in accordance with the literature. To a solution of 3-bromom-5-chloroaniline (1.0 eq) in DCM (0.1 M), was added (R)-5-oxo-1,4-thiazepane-3-carboxylic acid (1.0 eq), HOBt (1.5 eq), and DIC (1.2 eq) at rt. Reaction progress was monitored by TLC and upon completion, the reaction mixture was washed with water, concentrated, and redissolved in DMSO. The urea by product of DIC is poorly soluble in DMSO and will crash out of solution after 15 min. Crude DMSO solutions were filtered of the solid DIU byproduct and purified using a Gilson HPLC system (30 x 50 mm column; H2O with 0.1% TFA:acetonitrile). Fractions containing the desired product were quenched with saturated NaHCO3, extracted with 4:1 CHCl3:IPA, and concentrated to isolate the pure product as a white solid. 1H NMR (400 MHz, DMSO) δ 10.50 (s, 1H), 7.81 (t, J = 1.8 Hz, 1H), 7.72 (t, J = 1.9 Hz, 1H), 7.45 (t, J = 1.8 Hz, 1H), 7.19 (d, J = 6.7 Hz, 1H), 4.50 (ddd, J = 8.0, 6.6, 2.5 Hz, 1H), 3.04 (dd, J = 14.5, 2.5 Hz, 1H), 2.97 (dd, J = 14.5, 8.0 Hz, 1H), 2.90 – 2.74 (m, 2H), 2.70 (td, J = 4.9, 2.4 Hz, 2H). 13C NMR (101 MHz, DMSO) δ 174.77, 168.82, 141.41, 126.05, 122.54, 121.02, 118.53, 58.22, 40.79, 34.09, 23.88. LC-MS [m/z+H] = 362.9.